

Anomalous Micellization Behavior and Composition Heterogeneity of a Triblock ABA Copolymer of (A) Ethylene Oxide and (B) Propylene Oxide in Aqueous Solution

Zukang Zhou[†] and Benjamin Chu*

Chemistry Department, State University of New York at Stony Brook,
Long Island, New York 11794-3400. Received December 11, 1987;
Revised Manuscript Received March 8, 1988

ABSTRACT: Dynamic light scattering in combination with time-averaged scattered light intensity measurements has been employed to study the temperature-induced micellization behavior of poly(oxyethylene-oxypropylene-oxyethylene) block copolymer, poloxamer 184, in aqueous solution. As experimentally evidenced, there exist three temperature regions, namely, the unimer and micelle regions at the two extremes and an anomalous association behavior in the middle region which manifests itself with a milky opalescent appearance and a large angular dissymmetry in the scattered intensity before the onset of micellization. When filtration experiments are carried out to remove the "opalescent" minor components, the anomalous region is replaced by a normal transition region, where an equilibrium mixture of unimers and micelles occurs. Results of the composition analysis by NMR spectroscopy strongly support the composition heterogeneity mechanism for the anomalous association behavior. It has also been concluded that the presence of an anomalous association behavior requires, in addition to composition polydispersity, the phase separation of "impurities" to take place somewhere before the onset of micellization of the major component.

Introduction

Block copolymers of AB or ABA type, when dissolved in selective solvents which are thermodynamically good solvents for one type of block and precipitants for the other type of block, associate and form micelles¹ as a result of different solvation of the copolymer blocks and their incompatibility. In analogy to conventional amphiphiles, micellization of block copolymers obeys the closed association model,¹ which assumes a dynamic equilibrium between molecularly dispersed copolymer (unimer) and polymolecular aggregates (micelles). On the other hand, an anomaly in micellization which is usually absent in solutions of common detergents has been reported on a number of block copolymers in selective organic solvents or solvent mixtures. Examples are block copoly(styrene-methyl methacrylate) in toluene/furfuryl alcohol solvent mixture,² block copoly(styrene-butadiene styrene) in ethyl acetate³ or isopropyl acetate,⁴ block copoly(styrene-isoprene) in decane,⁵ and block copoly(styrene-2-vinylpyridine) in toluene.⁶ Recently, this type of anomalous behavior has also been observed on an aqueous system: block copoly(oxyethylene-oxypropylene-oxyethylene) in water.^{8,9} The so-called anomalous association behavior manifests itself essentially in the existence of a milky opalescent appearance with large angular dissymmetry in the scattered intensity before the onset of micellization. Possible explanations for the anomalous micellization in solutions of block copolymers in selective solvents have been discussed in many papers.²⁻⁷ For example, Utiyama et al.² claimed that in solutions of the diblock copolymer poly(styrene-methyl methacrylate) in the mixed solvent toluene/furfuryl alcohol, the polystyrene cores formed at the initial stages of micellization were anisotropic ellipsoids, which might result from the linear association of monomolecular micelles. A further deterioration of the solvent either by decreasing the temperature or by increasing the amount of the precipitant in the solvent mixture would change the micelles to spherical micelles with a compact core. Mandema et al.⁵ observed a maximum in the temperature dependence of the dissymmetry in the scattered

intensity for the diblock copolymer poly(styrene-isoprene) in decane and in the mixed solvent *trans*-decahydronaphthalene/decane. They concluded that in the region of large dissymmetry large particles with cylindrical or lamellae structures were presumably present. In discussing the anomalous behavior of block copoly(styrene-2-vinylpyridine) in toluene, Sikora and Tuzar⁶ speculated that the presence of either an insoluble homopolymer or a copolymer with a very high content of the insoluble component might be the reason. Thus, the origin for a distinct dissymmetry in the scattered intensity before the onset of micellization remains obscure and is open for discussion.

So far the micelle formation of poly(oxyethylene-oxypropylene-oxyethylene) block copolymers in aqueous solution has been the subject of controversy. For example, McDonald and Wong¹⁰ reported that no aggregation was noted at 25 °C for poloxamer 184 in water, whereas aggregation occurred at higher temperatures. However, recently Al-Saden et al.¹¹ concluded that aqueous poloxamer 184 showed detectable aggregates at 25 °C even with sizes larger than those at 35 °C. Furthermore, they suggested that the mechanism of the association process at 25 and 35 °C for the aqueous system studied could be different, i.e., with the open association type present at 25 °C and the closed association one at 35 °C, respectively.

In a previous communication,⁹ we briefly reported that, by carrying out a filtration experiment on an aqueous poloxamer 184 solution in the anomalous region, we were able to eliminate the anomalous micellization behavior, and correspondingly, a normal association behavior was observed instead. Therefore, our filtration results suggest that the heterogeneity in composition seems to be responsible for the anomaly in micellization of the block copolymers studied. Dynamic light scattering in combination with integrated scattered light intensity measurements has proved very useful in characterizing macromolecular or micellar systems. In this paper, static and dynamic light scattering studies on the association behavior in aqueous solutions of poly(oxyethylene-oxypropylene-oxyethylene) block copolymer, poloxamer 184, are presented, with our attention being concentrated on the anomalous behavior. It is unambiguously concluded that the anomalous association behavior can be ascribed to the composition polydispersity of the block copolymer, as

* Author to whom correspondence should be addressed.

[†] On leave from Chemistry Department, Peking University, Beijing, The People's Republic of China.

strongly evidenced by the disappearance of the anomalous region after removing the minor insoluble components. The composition analysis by NMR spectroscopy indicated that after filtration the residue on the filter did have a higher oxypropylene content, thus providing convincing positive proof of the concept of composition polydispersity in order to elucidate the anomalous association behavior.

Experimental Section

Materials and Solution Preparation. Two commercial poloxamer 184 (also called Pluronic L64) samples, obtained from Fluka Co. and Polysciences Co, respectively, were used in this study without further purification. Poloxamer 184 contains approximately 40% by weight oxyethylene units, the nominal molecular weight being $\sim 2900 \text{ g mol}^{-1}$. Solutions at different concentrations were prepared either individually or by diluting a stock solution. For light-scattering measurements, aqueous solutions were first centrifuged at $\sim 17000g$ for 2 h and then filtered through Millipore filter GS (nominal pore size $0.22 \mu\text{m}$) directly into 17-mm-o.d. light scattering cells. Finally the cells with clarified solution were sealed under vacuum.

Refractive Index Increment. The refractive index increment dn/dc for poloxamer 184 in water was measured by using a Brice-Phoenix differential refractometer at two wavelengths, 436 and 546 nm, and at two temperatures, 25.0 and 50.0 °C, respectively. The $(dn/dc)_T$ value at 488 nm was calculated by interpolation and found to be 0.140 and 0.129 mL g^{-1} at 25.0 and 50.0 °C, respectively. Values at other temperatures were estimated either by interpolation or by extrapolation, assuming that the quantity dn/dc has a linear temperature dependence over the temperature interval (20–50 °C) studied.

Light-Scattering Measurements. We used a standard, laboratory-built light-scattering spectrometer¹² capable of both absolute integrated scattered intensity and photon correlation measurements at different scattering angles. A Spectra-Physics argon ion laser (Model 165) was operated at 488 nm with an output power in the 200–400-mW range, depending upon the scattered light intensity level of the sample solution. The cell was held in a brass thermostat block filled with refractive index matching silicone oil, the temperature constancy being controlled to within ± 0.02 °C. Static light-scattering measurements were performed at angles between 25° and 135°. In the unimer and micelle regions, the angular scattering envelopes obtained were symmetrical. When distinct dissymmetry in the scattered intensity occurred in the anomalous region, scattered intensity values were obtained by extrapolation to zero scattering angle. In the absence of intramolecular interference, the Debye equation applies in the dilute solution regime:

$$\frac{H(C - \text{cmc})}{R_{v,90}} = \frac{1}{M_w} + 2A_2(C - \text{cmc}) \quad (1)$$

where $H (= 4\pi^2 n_0^2 (dn/dc)^2 / N_A \lambda_0^4)$ is an optical constant with N_A , n_0 , and λ_0 being Avogadro's number, the refractive index of solvent, and the wavelength of light in vacuo, respectively. $R_{v,90}$ is the excess Rayleigh ratio at scattering angle $\theta = 90^\circ$ with vertically polarized incident and scattered beams, C is the concentration in g mL^{-1} , cmc is the critical micelle concentration in g mL^{-1} , M_w is the weight-average molecular weight of unimers or micelles, and A_2 is the second virial coefficient. The excess Rayleigh ratio, $R_{v,90}$, was determined from the measured excess relative scattered intensity using the known Rayleigh ratio of benzene.¹²

For block copolymers which are heterogeneous in chemical composition, eq 1 yields an apparent molecular weight¹³ rather than a true weight-average molecular weight. However, for the present study, eq 1 can be considered as providing a reliable measure of the weight-average molecular weight regardless of the refractive index of the solvent, since refractive indices of the two constituent blocks are close to each other, being equal to 1.4563 and 1.4495, respectively, at the sodium D line for PEO and PPO blocks.

The photoelectron count time correlation function was measured at scattering angle $\theta = 30^\circ$ with a Brookhaven BI-2030 64-channel digital correlator. In most cases we accepted only those autocorrelation functions where the measured base line, i.e., the averaged value of the correlation function at very long delay times,

agreed with the computed base line to within $\sim 0.1\%$. At room temperatures the signal-to-noise ratio becomes relatively low due to the low scattered intensity. A few hours of accumulation were needed. The measured photoelectron count time correlation function in the self-beating mode has the form

$$G^{(2)}(\tau) = A(1 + b|g^{(1)}(\tau)|^2) \quad (2)$$

where $g^{(1)}(\tau)$ is the normalized electric field correlation function with τ being the delay time, A is the background, and b is a spatial coherence factor, usually taken as an adjustable parameter in the fitting procedure.

For a polydisperse solution,

$$|g^{(1)}(\tau)| = \int_0^\infty G(\Gamma) \exp(-\Gamma\tau) d\Gamma \quad (3)$$

where $G(\Gamma)$ is the normalized characteristic line-width distribution function with Γ being the characteristic line width. The mean characteristic line width $\bar{\Gamma}$ and the second moment μ_2 are defined by

$$\bar{\Gamma} = \int G(\Gamma) \Gamma d\Gamma \quad (4)$$

$$\mu_2 = \int G(\Gamma) (\Gamma - \bar{\Gamma})^2 d\Gamma \quad (5)$$

The cumulants method¹⁴ and the double-exponential fitting method¹⁵ were used for data analysis of the measured net intensity time correlation function $(Ab|g^{(1)}(\tau)|^2)$. For $qR < 1$ and q and R being the magnitude of the momentum transfer vector and the particle size, respectively, the mean line width ($\bar{\Gamma}$) is related to the z -average translational diffusion coefficient \bar{D} by the relation

$$\bar{\Gamma} = \bar{D}q^2 \quad (6)$$

Furthermore, in dilute solution the concentration dependence of the translational diffusion coefficient can be expressed adequately by a first-order expansion

$$\bar{D} = D_0(1 + k_d C) \quad (7)$$

where D_0 is the z -average diffusion coefficient at infinite dilution and k_d is the diffusion second virial coefficient. The corresponding hydrodynamic radius $R_{h,0}$ can then be calculated by using the Stokes-Einstein relation

$$R_{h,0} = k_B T / (6\pi\eta D_0) \quad (8)$$

Results and Discussion

1. Three Temperature Regions in Micellization.

For the polyol-type nonionic surfactants, the hydrophilic-hydrophobic characteristics of the surfactant molecules can be modified considerably by simply changing the temperature. Accordingly, in order to follow the temperature-induced micellization behavior in the aqueous poloxamer 184 system, a temperature change from 20 to 53 °C (the clouding point is 59 °C for a 10% solution) has been covered in this work. The association process has been studied via the temperature dependence of either the scattered light intensity (I) or the apparent hydrodynamic radius (R_h) of the particles. Figure 1 shows the scattered intensity results for both Fluka and Polysciences products at a concentration $C = 20.4 \text{ mg mL}^{-1}$. It is evident that there exist three distinct regions on the temperature curves shown in Figure 1: (1) At room temperatures, where low and nearly constant scattered intensity is detected, essentially unimers are present, since the weight-average molecular weight obtained by extrapolating the intensity data to zero concentration, as will be seen later, is close to the nominal value of $\sim 2900 \text{ g mol}^{-1}$. (2) In the "high"-temperature region (above ~ 34 °C), the scattered light intensity becomes about 1 or 2 orders of magnitude more than that in the unimer region and exhibits a pronounced temperature dependence. Thus, most likely, intermolecular aggregation occurs and micelles are present in this region, and the aggregation number increases with

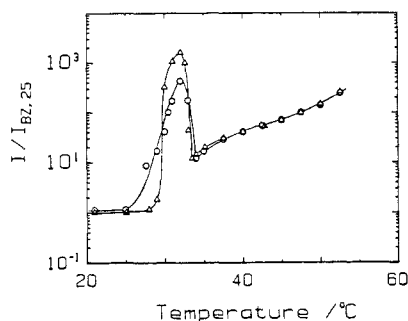


Figure 1. Plots of scattered light intensity relative to that of benzene at 25 °C ($I/I_{BZ,25}$) for poloxamer 184 in water as a function of temperature at concentration $C = 20.4 \text{ mg mL}^{-1}$. Circles denote Fluka product and triangles denote Polysciences product.

Table I
Static and Dynamic Properties of Poloxamer 184 in Water

temp, °C	M_w , g mol ⁻¹	A_2 , cm ³ mol g ⁻²	D_0 , cm ² s ⁻¹	$R_{h,0}$, nm
21.0	3200 ^a	7.8×10^{-4a}	1.3×10^{-6}	1.7
	3380 ^b	2.3×10^{-3b}		
25.0	3150 ^a	1.9×10^{-4a}	1.4×10^{-6}	1.7
	3380 ^b	2.0×10^{-3b}		
42.5	2.8×10^5a	7.2×10^{-4a}	3.6×10^{-7}	10.2
	2.8×10^5b	5.3×10^{-4b}		
47.5	7.2×10^5a	4.7×10^{-4a}	3.4×10^{-7}	12.0
	7.0×10^5b	4.5×10^{-4b}		
50.0	1.2×10^6a	3.2×10^{-5a}	2.9×10^{-7}	15.0
	1.1×10^6b	2.3×10^{-5b}		

^aFluka product. ^bPolysciences product. ^cIt should be noted that $R_{h,0}$ denotes the hydrodynamic radius at infinite dilution.

increasing temperature. (3) In the intermediate region where a typical anomalous micellization behavior is observed, the maximum scattered intensity is about 10^3 times more than that of the unimer region. Correspondingly, the dissymmetry ratio (I_{45}/I_{135}) reaches a high value of about 5.1 instead of being unity in both unimer and micelle regions. The abrupt increases suggest the presence of large particles with dimensions of the same order as the optical wavelength. It should be emphasized that while the two sample solutions in Figure 1 were prepared from different company sources, they showed almost the same temperature-dependence curve with minor differences in the height and width of the peak region. Therefore, such an association behavior seems to be a general characteristic of poloxamer 184 in water.

In order to have some deeper insight into the nature of the temperature-induced association process, we examined each of the three regions separately.

The Unimer Region. The static and dynamic solution properties, derived respectively from light-scattering intensity and line-width measurements, are summarized in Table I. The concentration range covered in the extrapolation procedure was from 4.92 to 20.4 mg mL⁻¹. To use eq 1, the critical micelle concentration (cmc) values were taken from a previous article.⁷ As shown in Table I, for the Fluka product the weight-average molecular weight values are almost the same at 21 and 25 °C, i.e., $M_w = 3.2 \times 10^3$ and $3.15 \times 10^3 \text{ g mol}^{-1}$, respectively. The corresponding M_w values for the Polysciences product are $3.38 \times 10^3 \text{ g mol}^{-1}$ at these two temperatures. The values are in good agreement with those reported by McDonald and Wong¹⁰ on the same aqueous system, but from a different source (Wyandotte Chemical Co.): $M_w = 3.09 \times 10^3 \text{ g mol}^{-1}$ at 25 °C. All these data by different sources suggest that at room temperatures poloxamer 184 is present essentially as unimers in aqueous solution. The second virial coefficient (A_2) can be considered as a measure of solute-

solvent and solute-solute interactions. Relatively large positive values of A_2 at room temperatures indicate that pronounced solute-solvent interactions occur, mainly due to hydrogen bond formation between ether oxygen atoms and water molecules. Therefore, no association occurs at room temperatures in this aqueous system.

On the basis of light-scattering line-width measurements in the temperature interval 21–25 °C, as indicated in Table I, small particles of an average size $R_h \sim 1.7 \text{ nm}$ but with a broad polydispersity were detected, the latter being explicitly indicated by the relatively large variance (μ_2/\bar{I}^2) of ~ 0.3 . Both the heterogeneity in chemical composition and the molecular weight distribution may account for the polydispersity in particle size. Assuming a sphere model, the hydrodynamic radius could also be estimated from the intrinsic viscosity data, using the following expression:

$$[\eta] = \frac{10\pi R_h^3 N_A}{3M} \quad (9)$$

where $[\eta]$ is the intrinsic viscosity and R_h is the radius of spheres which are equivalent to the dispersed copolymer molecules in respect to intrinsic viscosity. As we reported elsewhere,⁸ the R_h value for poloxamer 184 in water at 25 °C is 1.8 nm, which agrees well with that deduced from the diffusion coefficient in this work.

The Micelle Region. In the high-temperature region, as listed in Table I, the molecular weight values obtained are of the order of 10^5 – 10^6 and the hydrodynamic radius values derived at infinite dilution are about 6–9 times larger than those in the unimer region. Therefore, the high-temperature region corresponds to systems containing practically only polymolecular micelles. It should be noted that the lower boundary temperature of the micellar region is strongly concentration dependent, which shifts toward lower temperatures with increasing concentration, as can be seen later in Figure 6. The upper boundary is limited by the corresponding clouding point, beyond which phase separation would occur. For poloxamer 184 in water, the micellar molecular weight increases exponentially with increasing temperature, whereas in aqueous solutions of poloxamer 188 a linear temperature dependence has been detected.¹⁶ In addition, in the former case the micelle size becomes larger on raising the temperature, whereas in the latter case the micelle size remains almost constant as the temperature is increased. A similar exponential dependence of micellar molecular weight on temperature has been reported on a series of homologous nonionic detergents¹⁷—*n*-alkylhexaoxyethylene glycol monoethers (C_nE_6) with *n* being equal to 10–16. The only exception was C_8E_6 which was the most hydrophilic one among them and showed a linear temperature dependence in the temperature interval 18–30 °C. With respect to chemical composition, poloxamer 184 has the same average length of the middle hydrophobic block as poloxamer 188 but has a much shorter hydrophilic block at each side. Accordingly, in comparison with poloxamer 188 under the same conditions, poloxamer 184 has an enhanced tendency to separate from the solvent environment, thus making the aggregation number and also the micelle size larger, but becomes more sensitive to the temperature change. An alternative approach, perhaps, is to consider the clouding point as a reference. It may be expected that, since the temperature interval involved is relatively close to the clouding point (its values being 59 and 109 °C, respectively, for poloxamers 184 and 188), a similar behavior of exponential dependence on temperature would be found for poloxamer 188, although the latter is more hydrophilic in nature.

Table II
Estimated Values of Weight-Average Aggregation Number \bar{n} , Hydrodynamic Radius $R_{h,0}$, Core Radius r_{core} , and Shell Thickness d for Poloxamer 184 in Water

temp, °C	\bar{n}	r_{core} , nm	$R_{h,0}$, ^a nm	d , nm
42.5	88	3.9	10.2	6.3
47.5	225	5.4	12.0	6.6
50.0	356	6.3	15.0	8.7

^a It should be noted that $R_{h,0}$ denotes the hydrodynamic radius at infinite dilution.

In a previous article¹⁶ we reported that, for poloxamer 188 in water, the variance ($\mu_2/\bar{\Gamma}^2$) estimated from light-scattering line-width measurements has a value <0.1 (more often, ~ 0.05) in the micelle region, even though the unimers show a broad polydispersity in particle size. For poloxamer 184 in water, the polymolecular micelles also have a narrower size distribution than that of unimers, as indicated by the $\mu_2/\bar{\Gamma}^2$ values of ~ 0.04 – 0.08 instead of ~ 0.3 in the unimer region. This is again in accordance with the prediction made by Elias¹⁸ on the basis of a closed association model.

In poloxamer 184 the middle poly(oxypropylene) (PPO) block has a molecular weight of $\sim 1.75 \times 10^3$ g mol⁻¹ and is water insoluble. Therefore, PPO functions to form the core when micelle formation occurs. Assuming that block copolymer micelles are spherical in shape and contain liquidlike cores, we can estimate the core volume V_c or core radius r_{core} as follows:

$$V_c = \frac{4}{3}\pi r_{\text{core}}^3 = 30\bar{n}v_{\text{PO}} \quad (10)$$

and

$$v_{\text{PO}} = M_o/(\rho N_A) \quad (11)$$

where \bar{n} is the weight-average aggregation number, v_{PO} is the mean volume per PO unit within the core, M_o is the molecular weight of oxypropylene monomer, and ρ (taken as 1.01 g cm⁻³) is the density of liquid poly(oxypropylene). This estimate neglects the possible penetration of water and PEO into the micelle core and therefore gives a lower limit for the core size. The numerical difference between the measured hydrodynamic radius ($R_{h,0}$) and the estimated core radius (r_{core}) yields, to a first approximation, a shell thickness, d . The weight-average aggregation number (\bar{n}) and the hydrodynamic radius ($R_{h,0}$) together with the core radius (r_{core}) and the shell thickness (d) estimated at the corresponding temperatures are listed in Table II.

There exist two models to represent the configuration of the oxyethylene chain.¹⁹ One is the "zigzag" model, in which the chain is fully extended and the length and width of the oxyethylene unit amounts to 3.6 and 2.5 Å, respectively. The other one is the "meander" model, in which the chain is twisted into an expanded helical coil form with the corresponding length and width being 2.0 and 4.5 Å, respectively. As indicated in Table II, the estimated shell thickness is larger than the length of the side PEO block (on average, each containing 13 EO units) which is equal to 4.7 nm only, even if the chain is fully extended. However, even in the case of conventional surfactants, the extent of water penetration into the micellar core has been the subject of much controversy, so we will not go further into detailed discussion. It has been concluded by some authors¹⁹ that in aqueous solution poly(oxyethylene) chains are transformed to the meander configuration when the degree of polymerization is above ~ 10 , whereas in bulk the transformation to the meander configuration occurs at a degree of polymerization of ~ 20 – 40 . Besides, with

surface-active derivatives of poly(oxyethylene) the transformation is dependent on the hydrophobic base. Therefore, it seems reasonable and safe to consider the micelles formed in aqueous poloxamer 184 solution as consisting of a swollen poly(oxypropylene) core and a protective shell of poly(oxyethylene) chains in the zigzag configuration with some physically bound water molecules.

2. Anomalous Micellization Behavior. As a rule, the anomalous region exists in a relatively narrow range between the two temperature intervals corresponding to the unimer and micelle regions, respectively. If we take a closer look at the focused laser beam in the scattered medium with a traveling microscope, at the two extremes in temperature, i.e., in the unimer and micelle regions, the laser beam in the forward direction looks smooth and uniform, but with considerably stronger scattering in the latter case. Accordingly, in these two regions the intensity data are reproducible, and it is also possible to use a routine extrapolation procedure to determine the molecular weight or hydrodynamic radius of the corresponding dispersions. However, the situation is quite different in the middle transition region. At the very beginning, a few bright spots were seen on a uniform background. These spots were definitely not the "dust" particles from external sources, since they disappeared upon a moderate cooling back to the unimer region. Then, the number of speckles became more and more with increasing temperature. Also, the dissymmetry in the scattered intensity became larger. As we approached the peak position in Figure 1, the light beam appeared to have passed through a very dense colloidal (like ground glass) suspension. Thus, multiple scattering could occur with our present setup, and the results in the anomalous region, especially those near the peak, must necessarily be qualitative in nature. After having reached the maximum scattering intensity which was usually about 3 orders of magnitude larger than that in the unimer region, the scattered light intensity and number of spots were reduced dramatically upon a slightly further increase in temperature, say, only about half a degree. At the same time, the characteristic decay time in light-scattering line-width measurements decreased by a factor of ~ 20 – 30 . Finally, when the micelle region was encountered, the light beam in the scattering medium turned uniform again. Accordingly, the appearance of the anomalous region seems to be associated with some form of phase separation of the minor components in the composition inhomogeneous block copolymer. Some model calculations²⁰ show that, even in the case of a copolymer with a narrow distribution of molecular weight, the chemical heterogeneity could be appreciable. It means that heterogeneity in chemical composition is common for block copolymers. Therefore, composition heterogeneity may be the reason for the existence of the anomalous region in the micellization process.

In principle, we cannot exclude the possibility that the anomalous behavior might be an inherent property of block copolymers. For instance, Canham et al.³ published some electron micrographs obtained on the three block poly(styrene-butadiene-styrene) copolymer after removing the solvent (ethyl acetate) by evaporation. The micrographs show spherical particles of narrow size distribution under conditions corresponding to the micelle region and long, worm-like micelles under conditions corresponding to the occurrence of a maximum in the dissymmetry as a function of temperature. Then, it could be expected that these two forms of micelles should exist at equilibrium. There is also the other possibility that the large angular dissymmetry in the scattered intensity might be due to local concen-

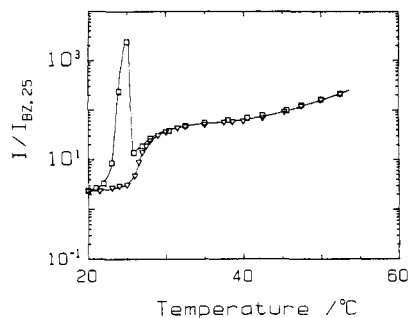


Figure 2. Effect of filtration on the temperature dependence of scattered light intensity for Polysciences poloxamer 184 in water. Solution concentrations are 100.0 and 98.6 mg mL⁻¹, respectively, before and after filtration. The filtration was performed at 25 °C by using Millipore VM filter with a nominal pore size of 500 Å. Squares denote before filtration and inverse triangles denote after filtration.

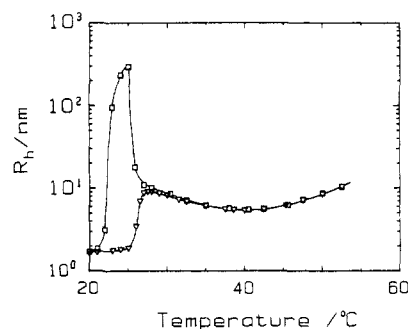


Figure 3. Effect of filtration on the temperature dependence of apparent hydrodynamic radius for Polysciences poloxamer 184 in water. Same filtration conditions and same symbols as in Figure 2.

tration fluctuations, but not due to the existence of very large aggregates.

In order to exclude the above two possible mechanisms, we designed a filtration experiment which was performed in close vicinity of the peak temperature. If the large angular dissymmetry were due to local concentration fluctuations, filtration could not separate the local temporal inhomogeneities in concentration and equilibrium would be reestablished on standing after filtration so that the anomalous behavior could not be eliminated. Alternatively, if the formation of large, anisotropic aggregates before the onset of micellization with consequential transformation to compact, spherical micelles was a characteristic of some block copolymers, then the equilibrium between the two forms of aggregates would disable the filtration process, because large aggregates should reappear in the filtrate. On the contrary, if our composition heterogeneity mechanism was correct, i.e., large particles could be formed by minor insoluble components, then after an effective filtration a normal micellization behavior should be observed on the temperature curve.

Figure 2 shows the scattered intensity results obtained on an aqueous poloxamer 184 solution (Polysciences product, $C = 100.0$ mg mL⁻¹) before and after filtration. The filtration was carried out at 25 °C (at the peak position) by using Millipore filter VM with a nominal pore size of 500 Å. Results of the corresponding apparent hydrodynamic radius obtained under the same conditions are shown in Figure 3. Both Figures 2 and 3 clearly indicate that after effective filtration the anomalous region has disappeared completely. Instead, as in the case of conventional nonionic amphiphiles, a normal transition region is observed. It should be noted that we have also performed a filtration experiment on the Fluka product at 34

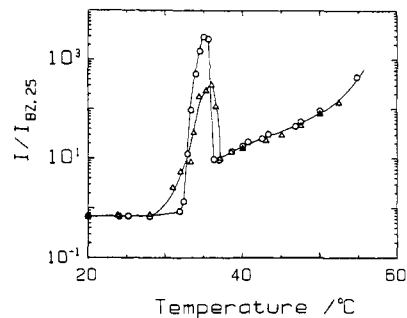


Figure 4. Effect of filtration on the temperature dependence of scattered light intensity for Fluka poloxamer 184 in water. The filtration was performed at 23 °C, i.e., in the unimer region, by using Millipore VM filter with a nominal pore size of 500 Å. Solution concentrations are 10.0 and 9.99 mg mL⁻¹, respectively, before and after filtration. Circles denote before filtration and triangles denote after filtration.

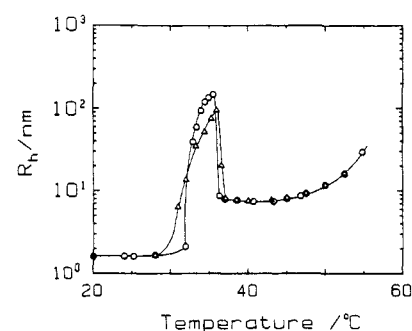


Figure 5. Effect of filtration on the temperature dependence of apparent hydrodynamic radius for Fluka poloxamer 184 in water. Same filtration conditions and same symbols as in Figure 4.

°C in the peak region ($C = 10.0$ mg mL⁻¹) and the corresponding anomalous behavior has also been eliminated. The details for the Fluka sample have been described in a short communication.⁹ Thus, using two samples from different commercial sources and working at two solution concentrations with a concentration difference of 1 order under conditions corresponding to each peak temperature, we have successfully eliminated the respective anomalous region. Next, we have carried out a similar filtration on the same Fluka solution ($C = 10.0$ mg mL⁻¹) under the same conditions as above except for the filtration temperature, which was chosen to be 23 °C, i.e., in the unimer region. Figures 4 and 5 show the results of the scattered intensity and of the apparent hydrodynamic radius, respectively, before and after filtration. Figures 4 and 5 clearly indicate that filtration operated in this manner, as could be expected, was ineffective to remove the peak region. The temperature curves of both I and R_h remained almost the same as before filtration, with only minor differences in the height and width of the peak region. From Figures 2 and 3 we have noticed that (1) all the peak regions end at the onset of normal micellization and (2) the removal of the anomalous region is accompanied by only a minor change in solution concentration. For example, the filtrate concentration for the Polysciences product is 98.6 mg mL⁻¹ as compared to the original value of 100.0 mg mL⁻¹ before filtration.

When all these experimental results are put together, a reasonably complete picture can be derived to interpret the anomalous association behavior in the following way. Block copolymers are more or less inhomogeneous in chemical composition. For poloxamer 184 in water, the minor components with lower oxyethylene contents, i.e., with larger hydrophobicity, would form large particles, not

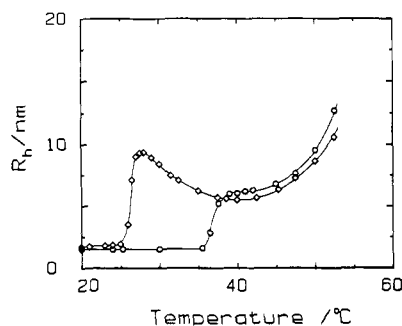


Figure 6. Plots of apparent hydrodynamic radius obtained for poloxamer 184 in water after effective filtration vs temperature at two different concentrations. Circles denote Fluka product at concentration of 9.65 mg mL⁻¹. Diamonds denote Polysciences product at concentration of 98.6 mg mL⁻¹.

far from the phase separation temperature which is below the critical micellization temperature (CMT) of the major component of the system studied. Here the major component means the central portion of the copolymer composition distribution. Upon raising the temperature, we first meet the phase separation of the minor insoluble components, which may lead to the formation of a dilute emulsion, as the droplets formed are stabilized by the adsorbed layer made up of the major component. As soon as the critical micellization temperature of the major component is reached, the insoluble minor components can either be incorporated into the cores of the micelles or form mixed micelles, depending on their molecular characteristics. Consequently, the temperature dependence of the scattered light intensity and the particle size would go through a maximum, as experimentally evidenced in our light-scattering measurements. Also, all the peak regions detected would end at the onset of micellization of the major component. Accordingly, the anomalous regions would then disappear after the removal of the insoluble minor components, as strongly evidenced in our filtration experiments. In general, as the temperature is increased, decreasing hydration occurs with the polyol-type nonionic surfactants. Therefore, for aqueous poloxamer solution, the CMT value shifts toward higher temperature with decreasing copolymer concentration. In the dilute solution regime, the phase separation temperature of nonionic surfactants also becomes higher with decreasing concentration. Thus, the anomalous region has been found experimentally to occur at higher temperature with decreasing copolymer concentration for the aqueous poloxamer system.

It is interesting to note that in the case of poloxamer 188, a more hydrophilic member in the series with approximately 80% by weight oxyethylene units, no anomaly in micellization has been detected in aqueous solution. Probably, the higher average oxyethylene content of poloxamer 188 results in $T_p > \text{CMT}$, where T_p is the phase separation temperature of the minor components with less EO units and CMT is the critical micellization temperature of the major component. As a result, on raising the temperature, we would first meet the micelle formation which masks the phase separation of the minor components by solubilization. Therefore, the presence of anomalous association behavior requires, in addition to composition heterogeneity, the phase separation of "impurities" to take place somewhere before the onset of micellization of the major component.

After the removal of the insoluble minor components, the normal transition region in the temperature-induced micellization process is clearly shown in Figure 6, where

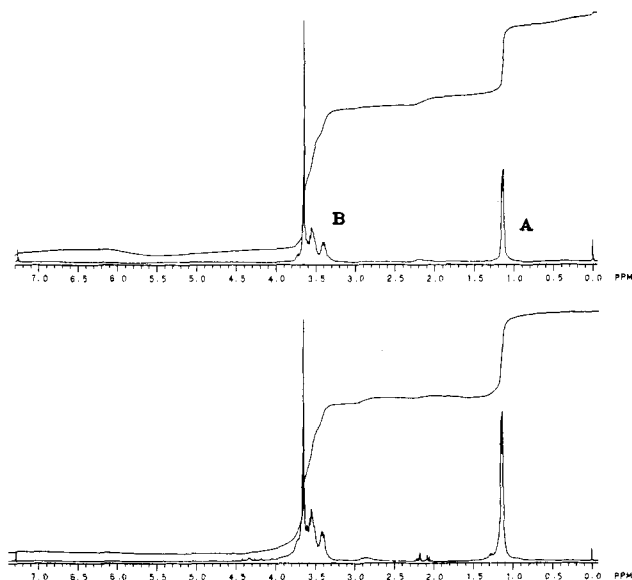


Figure 7. (a, top) ¹H NMR spectrum of Polysciences poloxamer 184 in CDCl₃ at 20 °C. (b, bottom) ¹H NMR spectrum obtained for the poloxamer 184 residue in CDCl₃.

the plots of apparent hydrodynamic radius obtained after effective filtration vs temperature at two largely different concentrations (9.65 and 98.6 mg mL⁻¹, respectively) are given. Figure 6 shows that the transition region covers a narrow temperature range of only 3–5 °C, the width becoming even narrower as the concentration increases. Also, its lower and upper boundaries are strongly concentration dependent. The curve shape in this region suggests that a dynamic equilibrium is established between individual unimers and polymolecular micelles, which shifts pronouncedly toward micelles with increasing temperature. Therefore, a mixture of unimers and micelles occurs in the transition region. However, in this region the equilibrium also shifts in favor of micelle formation as the concentration is increased. Thus, this kind of shift makes it impossible to determine quantitatively the molecular weight or hydrodynamic size of the micelles in the transition region, not even to mention their temperature dependence. At high copolymer concentration, for example, $C = 100$ mg mL⁻¹, the intermicellar interactions become important in addition to the decreasing hydration and increasing aggregation number of the micelles with rising temperature. A comprehensive consideration of all those factors involved may account for the complexity in the temperature dependence of the apparent hydrodynamic radius of micelles formed beyond the transition region, i.e., the appearance of the valley in the temperature curve, as shown in Figure 6.

3. Composition Analysis by NMR Spectroscopy. NMR spectroscopy provides a reliable method for the determination of the weight ratio of oxyethylene and oxypropylene in the poloxamer. If the composition heterogeneity mechanism for the anomalous micellization behavior is correct, we could predict that, after effective filtration in the anomalous region, the residue left on the filter should have a higher oxypropylene content as compared to that of the original sample, while the filtrate which has passed through the Millipore filter would be slightly richer in oxyethylene content. The 300-MHz ¹H spectrum was obtained, using a General Electric QE-300 spectrometer. Figure 7a shows the ¹H NMR spectrum obtained from the original Polysciences poloxamer 184 examined as a ~2% solution in CDCl₃ with tetramethylsilane as the internal reference compound. Figure

Table III
Results of Composition Analysis by NMR Spectroscopy

item	wt % of oxyethylene units
Polysciences poloxamer 184 before filtration	39.0
after filtration	
residue on filter	29.0
filtrate	41.6

7b shows the corresponding NMR spectrum obtained from the residue left on the filter. The residue was obtained under the same filtration conditions as shown in Figure 2 and then dissolved in cold water to form a clear solution consisting of unimers. The aqueous solution was then dried by evaporation to a constant weight and finally dissolved in an appropriate amount of CDCl_3 for NMR measurements.

The spectrum contains essentially two resonances: (A) the doublet centered at 1.12 ppm due to the methyl groups of the oxypropylene units; (B) a composite band from 3.3 to 3.9 ppm due to CH_2O groups of the oxyethylene and oxypropylene units and also the CHO group of the oxypropylene units. The resonance due to the hydroxyl group protons, which terminate the copolymer chain, also occurs in band B. The composition of poloxamer copolymer can be obtained readily from the relative areas of bands A and B, and we have

$$\frac{S_A}{S_B} = \frac{3b}{4a + 3b} \quad (12)$$

where S_A and S_B are the areas of bands A and B, respectively, and a and b are the mole fractions of EO and PO units in the copolymer analyzed, respectively. The weight percentage of EO units in the copolymer can be calculated by using the following relations:²¹

$$\% \text{EO} = \frac{33\beta}{33\beta + 58} 100 \quad (13)$$

and

$$\beta = \frac{S_B}{S_A} - 1 \quad (14)$$

The values of weight percentage of EO units in Polysciences poloxamer 184, determined before and after filtration, are listed in Table III. As seen from Table III, the EO content determined before filtration agrees well with the nominal value of 40%. In particular, the composition data listed strongly support the concept of composition heterogeneity as a mechanism for the anomalous association behavior of the copolymer investigated.

In addition, light-scattering intensity measurements were performed on an aqueous solution which was prepared by dissolving the residue in cold water, the concentration being 1.37 wt %. The intensity results are given in Figure 8. As shown in Figure 8, below $\sim 24^\circ\text{C}$, low, nearly constant scattered intensity was detected, and the corresponding apparent hydrodynamic radius was estimated to be 1.6 nm from line-width measurements, indicating that, most likely, unimers were present in solution. Upon a slight increase in temperature of only about 1 deg, the scattered intensity was dramatically increased by a factor of hundreds (or thousands) and a milky opalescence was observed. When the temperature reached 32°C , phase separation into two layers occurred. Such a striking behavior, characteristic of the residue, i.e., the insoluble minor components, again convincingly demonstrates the correctness of the composition heterogeneity mechanism

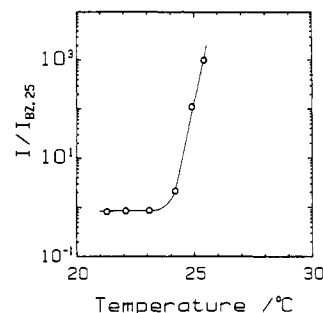


Figure 8. Temperature dependence of scattered light intensity relative to that of benzene at 25°C for 1.37 wt % aqueous solution of the poloxamer 184 residue left on the Millipore VM filter after effective filtration.

for the anomalous association behavior of block copolymer.

Conclusions

We have observed three regions in the temperature-induced micellization process for an ethylene oxide-propylene oxide ABA block copolymer, poloxamer 184, in water, i.e., the unimer and micelle regions at the two extremes and the anomalous association behavior in the middle region. After removal of the more hydrophobic minor components, the anomalous region is replaced by a normal transition region, where the equilibrium mixture of unimers and micelles occurs. As strongly evidenced by both NMR spectroscopy and light-scattering measurements on the residue, it is unambiguously concluded that the anomalous micellization behavior can be ascribed to the composition heterogeneity of the block copolymer studied.

Acknowledgment. We gratefully acknowledge support of this research by the U.S. Army Research Office, Chemical and Biological Sciences Division (DAAL03-87-K-0136) and the National Science Foundation (INT8619977). We wish to thank Zhaoda Zhang for his help in NMR measurements.

Registry No. Poloxamer 184, 106392-12-5.

References and Notes

- (1) Tuzar, Z.; Kratochvil, P. *Adv. Colloid Interface Sci.* **1976**, *6*, 201.
- (2) Utiyama, H.; Takenaka, K.; Mizumori, M.; Fukuda, M.; Tsunashima, Y.; Kurata, M. *Macromolecules* **1974**, *7*, 515.
- (3) Canham, P. A.; Lally, T. P.; Price, P.; Stubbersfield, R. B. *J. Chem. Soc., Faraday Trans. 1* **1980**, *76*, 1857.
- (4) Tuzar, Z.; Sikora, A.; Petrus, V.; Kratochvil, P. *Makromol. Chem.* **1977**, *178*, 2743.
- (5) Mandema, W.; Zeldenrust, H.; Emeis, C. A. *Makromol. Chem.* **1979**, *180*, 1521, 2163.
- (6) Sikora, A.; Tuzar, Z. *Makromol. Chem.* **1983**, *184*, 2049.
- (7) Tuzar, Z.; Bahadur, P.; Kratochvil, P. *Makromol. Chem.* **1981**, *182*, 1751.
- (8) Peng, X.; Zhou, Z. *Acta Chim. Sinica* **1986**, *44*, 613.
- (9) Zhou, Z.; Chu, B. *Macromolecules* **1987**, *20*, 3089.
- (10) McDonald, C.; Wong, C. K. *J. Pharm. Pharmacol.* **1974**, *26*, 556.
- (11) Al-Saden, A. A.; Whateley, T. L.; Florence, A. T. *J. Colloid Interface Sci.* **1982**, *90*, 303.
- (12) Chu, B.; Onclin, M.; Ford, J. R. *J. Phys. Chem.* **1984**, *88*, 6566.
- (13) Bushuk, W.; Benoit, H. *Can. J. Chem.* **1958**, *36*, 1616.
- (14) Koppel, D. E. *J. Chem. Phys.* **1972**, *57*, 4814.
- (15) Chu, B.; Ford, J. R.; Dhadwal, H. S. *Methods Enzymol.* **1985**, *117*, 256.
- (16) Zhou, Z.; Chu, B. *J. Colloid Interface Sci.*, in press.
- (17) Balmbra, R. R.; Clunie, J. S.; Corkill, J. M.; Goodman, J. F. *Trans. Faraday Soc.* **1964**, *60*, 979.
- (18) Elias, H.-G. *J. Macromol. Sci. Chem.* **1973**, *A7*, 601.
- (19) Rosch, H. In *Nonionic Surfactants*; Shick, M. J., Ed.; Marcel Dekker: New York, 1967.
- (20) Kotaka, T.; Donkai, N.; Ik Min, T. *Bull. Inst. Chem. Res., Kyoto Univ.* **1974**, *52*, 332.
- (21) Mathias, A.; Mellor, N. *Anal. Chem.* **1966**, *38*, 472.